International Symposium on Antennas and Propagation
27 – 30 October 2008, Taipei, Taiwan
Taipei International Convention Center

Ultra Wideband Small-Scale Amplitude Fading Statistics in Indoor Laboratory Environments

Roghieh Karimzadeh Baee, Narges Noori and Ali Abolghasemi
Iran Telecommunication Research Center, Tehran, Iran
Email: rkbaee@itrc.ac.ir, nnoori@itrc.ac.ir, ali_abl@itrc.ac.ir

1. Introduction

The use of ultra wideband (UWB) technology has recently attracted the intense interest of wireless system designers due to its potential in short range high data rate communications [1]-[3]. In a wireless system, the transmitted signal interacts with the physical environment in a complex manner. Therefore, a summation of several multipath components may arrive at the receiver. The ability to accurately model this complex phenomenon is crucial to systems design. The results of some UWB time or frequency-domain channel measurements and characterization at home, office and hospital environments have been presented in [4]-[7] for different frequency bands and transmitter-receiver separation distances. One of the fundamental parts of the channel characterization is the study of small-scale amplitude fading. The Rice and Rayleigh distributions can describe the amplitude fading statistics in conventional narrowband channel models for LOS and NLOS condition, respectively. In the UWB propagation, the wide frequency bandwidth corresponds to a high temporal resolution capability. Therefore, a single path arriving at a certain delay must be resolved. In order to evaluate the small-scale amplitude fading statistics, the empirical amplitudes over small-scale areas are calculated. Relative data from taps at specific excess delays were matched to some typical theoretical distributions for amplitude fading statistics such as Lognormal, Nakagami, Rayleigh, Rice, and Weibull distributions depending on the measurement environments and scenarios [3]. In [7]-[9] Lognormal distribution was obtained to give the best fit for the amplitude fading statistics, while other measurement campaigns such as [10, 11] show the small-scale amplitude fading statistics can be modelled by the Nakagami distribution. In [12] the Rice distribution had also best fitted to empirical data. The measurement results reported in [13]-[15] show that the small-scale amplitude fading have a good fit with weibull distribution for fully furnished conference room, a modern office building and high rise apartments, respectively.

In the present work, the results of ultra wideband time-domain measurements in the laboratory (Lab) environment are presented to investigate the small-scale amplitude fading statistics for both line of site (LOS) and non-LOS (NLOS) scenarios. The Lab environments are equipped with many electronic and measurement devices, made of metallic materials, which are located on tables. Therefore, the amplitude fading statistics in the Lab is different from the office and residential environments, where the most of the furniture are made from wood and textile products.

2. **UWB Time-Domain Measurements**

2.1 Measurement Setup

A diagram of the time-domain measurement setup is shown in Fig. 1. At the transmitter side, a pulse generator was used as an UWB signal source. The width of the transmitting pulse is less than 50 ps. This generator was connected to the transmitting antenna through a low loss wideband cable. The output signal of the receiving antenna was amplified by a low noise amplifier with a gain of 28 dB and 3 dB bandwidth of 12 GHz. A digital sampling oscilloscope was used at the receiver side which sampled the received signal at a rate of 1 sample per 12.5 ps. The pulse generator and the digital sampling oscilloscope were synchronized through a reference clock signal at a frequency of 200 kHz. Measurements were performed by a pair of 1-18 GHz double-ridged waveguide horn antennas. These transmitting and receiving antennas were both placed on moving carts at a height of 135 cm above ground.

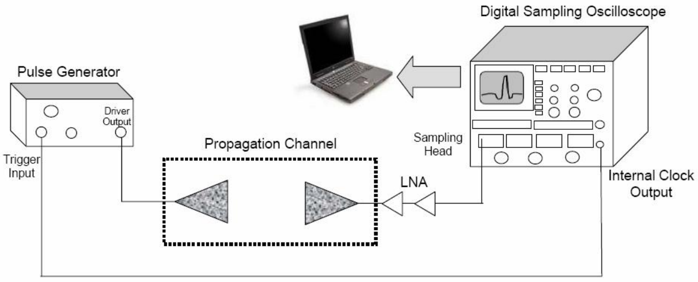

Figure 1: A diagram of the used time-domain measurement setup.

2.2 Measurement Location and Procedure

The time-domain measurement campaign was conducted for both LOS and NLOS scenarios at a basement floor with the plan shown in Fig. 2. All the main rooms of this floor are modern Labs. The building walls are made of brick with metallic stud. The partitions are aluminum frame structured with fabric, wood and glass surface. The floor of the rooms is covered with tiles. The doors are made of wood and have metallic frames. The furniture inside each room consists of many different electronic and measurement devices, metallic and wooden cupboards and cabinets, table made of wood, mid back work chairs, computers, etc.

Figure 2: Plan of the measurement environment with different Tx and Rx locations.

To perform the measurements, five different transmitter locations were considered. The receiver points were chosen at those locations where the received signal could be clearly detected. The measurements were collected at each receiver location by moving the receiver antenna over a square grid of 9 points spaced 50 cm apart as shown in Fig. 2. In order to cancel out the noise, 100 measurements were averaged at each measurement point. A system calibration was made to compensate any imperfection of the system components. Then any dc offset that had not been taken into account by the calibration was removed.

3. Amplitude Fading Statistics

In this section, small-scale amplitude fading statistics are extracted from the measurement data in the Lab environment. Empirical data of the power delay profiles (PDPs) from different measurement position are gathered and classified into LOS and NLOS. Amplitudes smaller than 35dB of the peak in each PDP are set to zero in order to get only the appropriate data for analysis.

Then, data from taps at specific excess delays are collected. Each tap is assumed to contain either one resolvable path or no path. This delay tap is determined by the time resolution of the specific measurement system [7], [13]. For our measurement system, the delay tap width is 12.5 ps. Extraction of the amplitudes for each tap is carried out by collecting a vector of amplitude values having same delay. It can be found that these data from taps at specific excess delays are matched to some typical theoretical distributions such as Lognormal, Nakagami, Weibull in which the parameters of these distributions i.e. the standard deviation of Lognormal distribution, *m*-parameter of the Nakagami distribution and *b*-shape parameter of the Weibull distribution are Lognormal distributed random variables, respectively [3]. Variations of these parameters as a function of excess delay are extracted from the measurement data for both LOS and NLOS scenarios and shown in Fig. 3. The mean value and standard deviation of the Lognormal distributed for these three parameters are also listed in Table 1.

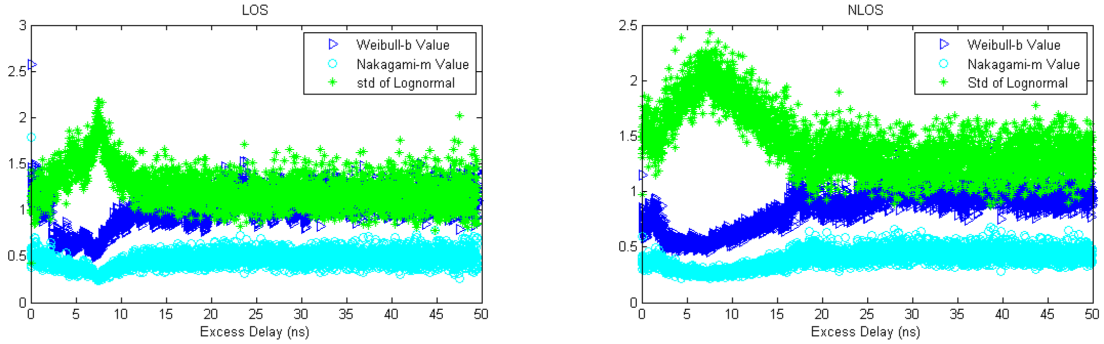

Figure 3: Variation of Lognormal distribution standard deviation, Nakagami *m*-parameter and Weibull *b*-shape parameter as a function of excess delay.

The Kolmogorov–Smirnov (K–S) and chi-square (c^2) hypothesis tests are used to elaborate the goodness-of-fit for these candidate amplitude distributions. A significance level of 5% is used to evaluate the reliability of the fit. Table 2 compares the passing rate of the K-S and c^2 tests for the above distributions. It is found from the table that the Weibull gives the highest passing rate in both tests. Therefore, it can be concluded that the small-scale amplitude fading statistics can be well-modeled by Weibull distribution for both scenarios. The CDFs of the empirical small-scale amplitude fading fitted to the Weibull distribution are plotted in Fig. 4 at 25 ns and 50 ns excess delays for LOS condition.

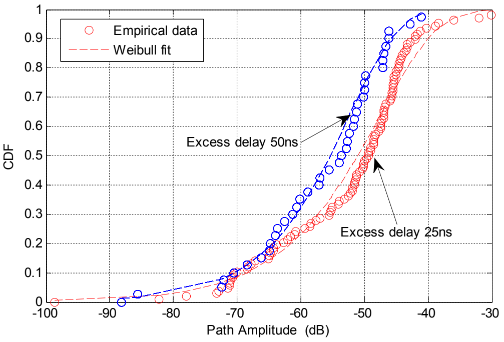

Figure 4: CDFs for the empirical small-scale amplitude fading fitted with Weibull distribution at different excess delay for LOS

Table 1: Mean and standard deviation of parameters for candidate distributions.

parameters	**σ-Lognormal**		**m-Nakagami**		**b-Weibull**	
	$\mu_{\sigma L}$	$\sigma_{\sigma L}$	μ_{mN}	σ_{mN}	μ_{bW}	σ_{bW}
LOS	1.2366	0.2009	0.4649	0.0811	1.1115	0.1711
NLOS	1.4397	0.2826	0.3973	0.0797	0.8886	0.1932

Table 2: Passing rate of K-S and c^2 hypothesis test.

Distribution	**LOS**		**NLOS**	
	K-S	c^2	K-S	c^2
Lognormal	84.85	46.16	97.6	75.29
Nakagami	50.95	52.83	25.68	33.38
Weibull	92.44	89.18	98.85	91.05

4. Conclusions

The results of time-domain UWB channel measurement in the Lab environment were presented to investigate the small-scale amplitude fading statistics in Lab environment for both LOS and NLOS conditions. It was shown that small-scale amplitude fading can be modeled by the Lognormal, Nakagami or Weibull distribution but Weibull distribution has maximum passing rate of the K-S and c^2 tests in both scenarios. The parameters of these distributions can be modeled by another Lognormal distribution.

Acknowledgments

The authors would like to express their sincere thanks to the staffs of the Communication Technology and Type Approval Lab for their contributions during the measurement campaign.

References

[1]. J.C. Adams, W. Gregorwich, L. Capots, and D. Liccardo, “Ultra-wideband for navigation and communications,” in Proc. IEEE Aerospace Conference, vol. 2, pp. 785-792, March 2001.

[2]. S. Gezici, Z. Sahinoglu, H. Kobayashi, and H. V. Poor, “Ultra-wideband impulse radio systems with multiple pulse types,” IEEE Journal on Selected Areas in Communications, vol. 24, no. 4, pp. 892 – 898, April 2006.

[3]. H. Arslan, Z. N. Chen, and M.-G. Di Benedetto, *Ultra Wideband Wireless Communications,* John Wiley & Sons, 2006.

[4]. S. S. Ghassemzadeh, R. Jana, C. W. Rice, W. Turin, and V. Tarokh, “Measurement and Modeling of an Ultra-Wide Bandwidth Indoor Channel,” IEEE Transactions on Communications, vol. 52, no.10, pp. 1786-1796, October 2004.

[5]. W. Ciccognani, A. Durantini and D. Cassioli, “Time domain propagation measurements of the UWB indoor channel using PN-sequence in the FCC-compliant band 3.6–6 GHz,” IEEE Transactions on Antennas and Propagation, vol. 53, no. 4, pp. 1542-1549, April 2005.

[6]. A. Muqaibel, A. Safaai-Jazi, A. Attiya, B. Woerner, and S. Riad, “Path-loss and time dispersion parameters for indoor UWB propagation,” IEEE Transactions on Wireless Communications, vol. 5, no. 3, pp. 550-559, March 2006.

[7]. L. Hentilä1, A. Taparungssanagorn, H. Viittala, and M. Hämäläinen, “Measurement and modelling of an UWB Channel at hospital,” in Proc. IEEE International Conference on Ultra-Wideband, pp. 113-117, September 2005.

[8]. J. R. Foerster and Q. Li, “UWB channel modeling contribution from Intel,” IEEE P802.15-02/279r0-SG3a, June 2002.

[9]. Q. Li and W. S. Wong, “Measurement and analysis of the indoor UWB channel,” in Proc. IEEE Vehicular Technologies Conf. (VTC 2003-Fall), Orlando, FL, September 2003, pp. 1–5.

[10].D. Cassioli, M. Z. Win, and A. F. Molisch, “The ultra-wide bandwidth indoor channel: from statistical model to simulations,” IEEE J. Select. Areas Commun., vol. 20, no. 6, pp. 1247–1257, August 2002.

[11]. F. Zhu, Z. Wu, and C. R. Nassar, “Generalized fading channel model with application to UWB,” in Proc. IEEE Conf. UWB Systems and Technologies (UWBST02), Baltimore, MD, May 2002, pp. 13–18.

[12]. J. Kunisch and J. Pamp, “Measurement results and modeling aspects for the UWB radio channel,” in Proc. IEEE Conf. UWB Systems and Technologies (UWBST02), Baltimore, MD, May 2002, pp. 19–23.

[13]. C.-C. Chong, and S. K. Yong, “A Generic Statistical-Based UWB Channel Model for High-Rise Apartments,” IEEE Transactions on Antenna and Propagation, Vol. 53, No. 8, August 2005.

[14]. A. Alvarez, G. Valera, M. Loberia, R. Torres, and J. L. Garcia, “Ultrawideband channel characterization and modeling,” in Proc. Int. Workshop on Ultra Wideband Systems (IWUWBS 2003), Oulu, Finland, Jun. 2003.

[15]. P. Pagani and P. Pajusco, “Experimental assessment of the UWB channel variability in a dynamic indoor environment,” in Proc. IEEE Int. Symp. Personal, Indoor and Mobile Radio Commun. (PIMRC 2004), Barcelona, Spain, Sep. 2004, pp. 2973-2977.